

{(1*R*,2*R*,4*R*)-4-Methyl-1,2-cyclohexanediamine}oxalatoplatinum(II): A Novel Enantiomerically Pure Oxaliplatin Derivative Showing Improved Anticancer Activity in Vivo

Sergey A. Abramkin,[†] Ute Jungwirth,^{‡,⊥} Seied M. Valiahd, ^{†,⊥} Claudia Dworak,[†] Ladislav Habala,[†] Kristof Meelich,[†] Walter Berger,^{‡,§} Michael A. Jakupc,[†] Christian G. Hartinger,[†] Alexey A. Nazarov,^{*,||} Markus Galanski,^{*,†} and Bernhard K. Keppler^{*,†,§}

[†]University of Vienna, Institute of Inorganic Chemistry, Währinger Strasse 42, A-1090 Vienna, Austria, [‡]Department of Medicine I, Institute of Cancer Research, Medical University of Vienna, Borschkegasse 8a, A-1090 Vienna, Austria, [§]Research Platform “Translational Cancer Therapy Research” University of Vienna, Währinger Strasse 42, A-1090 Vienna, Austria, and ^{||}Institut des Sciences et Ingénierie Chimiques, Ecole Polytechnique Fédérale de Lausanne (EPFL), CH-1015 Lausanne, Switzerland. [⊥]U.J. and S.M.V. contributed equally to this work

Received May 20, 2010

Novel derivatives of the clinically established anticancer drug oxaliplatin were synthesized. Cytotoxicity of the compounds was studied in six human cancer cell lines by means of the MTT assay. Additionally, most promising complexes were also investigated in cisplatin- and oxaliplatin-resistant human cancer cell models. The therapeutic efficacy in vivo was studied in the murine L1210 leukemia model. Most remarkably, {(1*R*,2*R*,4*R*)-4-methyl-1,2-cyclohexanediamine}oxalatoplatinum(II), comprising an equatorial methyl substituent at position 4 of the cyclohexane ring, was as potent as oxaliplatin in vitro but distinctly more effective in the L1210 model in vivo at the optimal dose. The advantage observed in the in vivo situation was mainly based on a more favorable therapeutic index. The maximum tolerated dose of the novel analogue was higher than that of oxaliplatin and caused a greater increase in life span (>200% versus 152%), with more animals experiencing long-term survival (5/6 versus 2/6). These data support further (pre)clinical development of the methyl-substituted oxaliplatin analogue with improved anticancer activity.

Introduction

The cytotoxic properties of cisplatin, *cis*-diamminedichloridoplatinum(II),¹ were found by serendipity in Barnett Rosenberg's laboratory in 1965.^{2,3} Cisplatin was finally approved by the Food and Drug Administration (FDA⁴) in 1978. Exchange of the two chloride leaving groups of cisplatin with the more kinetically inert 1,1-cyclobutanedicarboxylato ligand resulted in carboplatin, *cis*-diammine(1,1-cyclobutanedicarboxylato)platinum(II), which received approval in 1989 as second-generation platinum-based agent. In 2004, the FDA approved the third generation platinum drug, oxaliplatin (Figure 1), {(1*R*,2*R*)-cyclohexanediamine}oxalatoplatinum(II),^{4,5} for the first line treatment of colorectal carcinoma in combination with 5-fluorouracil and leucovorin

(5-FU/LV); neurotoxicity was found to be dose limiting.⁶ Clinical trials based on different tumors of the gastrointestinal tract and breast and lung carcinomas are ongoing. Remarkably, oxaliplatin shows a different spectrum of cytotoxicity compared to *cis*- and carboplatin as deduced from the 60 cell line panel of the NCI, being in accord with its activity in the inherently *cis*- and carboplatin resistant colorectal carcinoma.⁷

Compared to cisplatin, the volume of distribution (serves as a measure, how effectively a drug is cleared from the bloodstream and going into tissue) of oxaliplatin is considerably high. Moreover, the terminal elimination phase is longer than that for cisplatin.⁸ The mechanism of cellular oxaliplatin accumulation is still unclear. In contrast to cisplatin, accumulation of oxaliplatin in cancer cells is less dependent on the copper transporter CTR1.⁹ Like cisplatin, the ultimate target of oxaliplatin is the genomic DNA and it forms the same types of inter- and intrastrand DNA cross-links as cisplatin,^{10,11} however, the reactivity toward isolated and cellular DNA is lower.¹² Because the cytotoxic potency of oxaliplatin is generally well comparable or even higher than that of cisplatin in some cell lines, oxaliplatin-induced DNA adducts have to be more cytotoxic than those arising from cisplatin.¹³ Cisplatin–DNA adducts are effectively recognized by the MMR complex and by HMG1 but not those adducts deriving from oxaliplatin.^{14,15} Postreplicative bypass is also different and more efficient past oxaliplatin–GG adducts.¹⁶ On a molecular level, the adducts of oxaliplatin¹⁷ and cisplatin¹⁸ with the same dodecamer duplex were investigated by crystal structure

*To whom correspondence should be addressed. For A.A.N.: phone, +41 (0)21 693 98 60; fax, +41 (0)21 693 98 85; E-mail, alexey.nazarov@epfl.ch, For M.G.: phone, +43-1-4277-52603; fax, +43-1-4277-52680; E-mail, markus.galanski@univie.ac.at. For B.K.K.: phone, +43-1-4277-52602; fax, +43-1-4277-52680; E-mail, bernhard.keppler@univie.ac.at.

^a Abbreviations: 5-FU, 5-fluorouracil; Cbz, carbobenzoxy; COSY, correlated spectroscopy; CTR, copper transporter; DACH, diaminocyclohexane; DMF, dimethylformamide; DMSO, dimethyl sulfoxide; d-OHP, *S,S*-enantiomer of oxaliplatin; ESI, electrospray ionization; FDA, Food and Drug Administration; G, guanine; HMG, high-mobility group protein; ILS, increase in life span; LV, leucovorin; MEM, minimal essential medium; MMR, mismatch repair; MsCl, methanesulfonyl chloride; MTD, maximum tolerated dose; MTT, 3-(4,5-dimethyl-2-thiazolyl)-2,5-diphenyl-2*H*-tetrazolium bromide; NCI, National Cancer Institute; Py, pyridine.

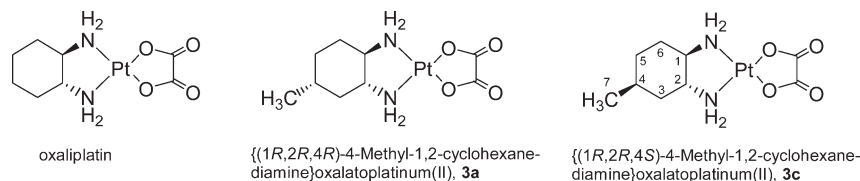


Figure 1. Structures of oxaliplatin and the novel enantiomerically pure oxaliplatin derivatives with either equatorial (**3a**) or axial (**3c**) methyl substituent with NMR numbering scheme.

diffraction, revealing a relatively similar geometry. From that point of view, it is difficult to understand the differences in their cytotoxic potential. However, it has to be taken into account that the situation in solution may vary from that in the solid state as could be demonstrated recently.¹⁹

The cyclohexanediamine carrier ligand in oxaliplatin comprises a *trans*-1*R*,2*R* configuration with both amino substituents in equatorial position; the cyclohexane ring is situated nearly perfectly within the square planar coordination plane.²⁰ The same holds true for the *trans*-1*S*,2*S* enantiomer. In the case of the *cis*-1*R*,2*S* counterpart, one amino substituent is in an equatorial and the other in an axial position, leading to a nearly perpendicular arrangement of the cyclohexane ring with respect to the coordination plane.²¹ The antiproliferative properties of all three (cyclohexanediamine)-oxalatoplatinum(II) complexes have been investigated with the following structure–activity relationship (DACH = diaminocyclohexane): *trans*-1*R*,2*R*-DACH enantiomer > *trans*-1*R*,2*R*/1*S*,2*S*-DACH racemate > *trans*-1*S*,2*S*-DACH enantiomer > *cis*-1*R*,2*S*-DACH diastereomer.^{22,23} The difference between *trans*- and *cis*-configured complexes is easily explainable by the shape of the *cis* analogue (perpendicular arrangement of the cyclohexane ring). Indeed, due to steric hindrance, adduct formation with DNA was slow and also the conversion of the monoadduct to the bisadduct.²⁴ However, in the case of both *trans*-isomers (same shape), the DNA seems to act as chiral discriminator as could be shown by Lippard and colleagues.¹⁷ Formation of a hydrogen bond between the pseudoequatorial NH hydrogen of the (1*R*,2*R*)-cyclohexanediamineplatinum(II) fragment and O⁶ of a neighboring guanine was found, which is not possible in the case of *trans*-1*S*,2*S*-configuration.

Finally, what we really do know about the mode of action of oxaliplatin and what may serve as basis for the development of novel oxaliplatin derivatives with improved cytotoxic and anticancer properties are: (i) distribution in the body and cellular accumulation of cisplatin and oxaliplatin are different and (ii) recognition and processing of DNA adducts are not the same. These features are, at least in part, the result of the *trans*-(1*R*,2*R*)-cyclohexanediamine carrier ligand, providing lipophilicity along with steric bulk to oxaliplatin. Consequently, we have focused on further increasing the lipophilicity/steric bulk of the cyclohexanediamine moiety. Here, we report for the first time on the synthesis, characterization, in vitro cytotoxicity, and in vivo anticancer activity of a novel enantiomerically pure oxaliplatin derivative, {(1*R*,2*R*,4*R*)-4-methyl-1,2-cyclohexanediamine}oxalatoplatinum(II), exhibiting an equatorial methyl group at position 4 of the cyclohexane ring. We also demonstrate that bigger substituents (ethyl or *t*-butyl) do not lead to an improvement of the cytotoxic and anticancer properties.

Results and Discussion

The aim of the present work was to synthesize close analogues of oxaliplatin, which are equipped with an

increased lipophilicity, additionally having an influence on the structure of adducts formed with the final target DNA. Consequently, the intention was to improve the biological properties of oxaliplatin and not to develop completely different types of complexes (“The most fruitful basis for the discovery of a new drug is to start with an old drug” Sir James Black, Nobel Prize in Physiology or Medicine in 1988).²⁵ The oxalato leaving group was left unchanged because it affects the solubility, the biodistribution, and the systemic toxicity but of course not the structure of DNA adducts. The {*trans*-(1*R*,2*R*)-cyclohexanediamine}platinum(II) fragment binds to DNA in the major groove (Supporting Information, Figure S1), generating there an unpolar region/steric bulk. From that point of view, it seems to be reasonable to derivatize the fragment at position 4 of the cyclohexane ring (preferably in equatorial position), offering a maximal distance from the coordination site. Substitution at positions close to the metal center, or even at the coordinated nitrogen atoms, would significantly influence the structural changes of DNA adducts and were therefore not favored.

Synthesis and Characterization. Racemic (1*R*,2*R*,4*R*/1*S*,2*S*,4*S*)-4-methyl-1,2-cyclohexane-diamine was synthesized as reported recently.²⁶ Shortly, 4-methylcyclohex-1-ene was converted into the vicinal *trans*-diol (Scheme 1) by treatment with hydrogen peroxide in the presence of formic acid. In a next step, the corresponding mesylate was formed via reaction with methanesulfonyl chloride/pyridine, which was then transferred with sodium azide into 4-methyl-*trans*-1,2-cyclohexanediazide. The diamine was subsequently obtained by reduction with hydrogen at Pd on CaCO₃ (Lindlar’s catalyst).

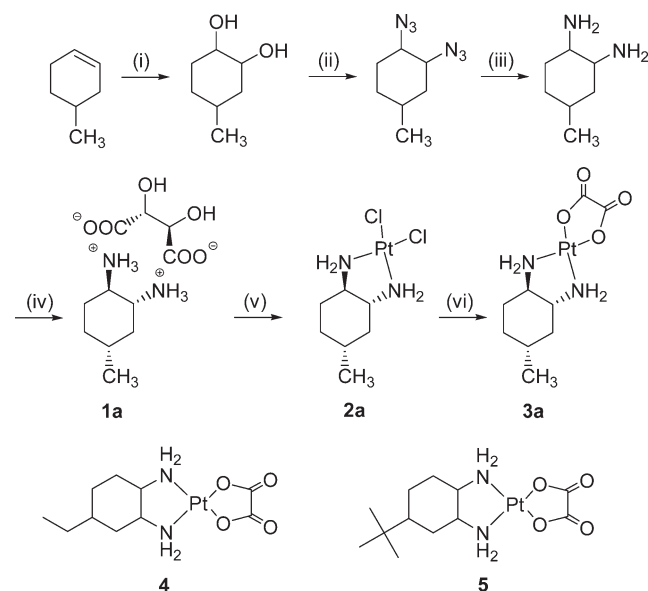
Enantiomer separation of racemic (1*R*,2*R*,4*R*/1*S*,2*S*,4*S*)-4-methyl-1,2-cyclohexanediamine was performed via recrystallization of the respective L- or D-tartrates in an ethanol–water mixture (Supporting Information, Scheme S1). Enantiomeric purity was proven by chiral HPLC. Prior to HPLC analysis, the diamines were derivatized with benzyloxycarbonyl chloride in order to obtain UV-active compounds (**6** + **7**, Supporting Information, Scheme S1 and Figure S2).

Enantiomerically pure (1*R*,2*R*,4*R*)-4-methyl-1,2-cyclohexanediaminium L-tartrate, **1a**, was then reacted with K₂PtCl₄ in the presence of NaOH, resulting in the yellow dichloridoplatinum(II) complex **2a**. The chlorido ligands were released with AgNO₃ and addition of potassium oxalate to the formed diaquaplatinum(II) species finally resulted in the white target complex **3a**, {(1*R*,2*R*,4*R*)-4-methyl-1,2-cyclohexanediamine}oxalatoplatinum(II). The corresponding 1*S*,2*S*,4*S*-enantiomer **3b** was obtained by following the same procedure and starting from (1*S*,2*S*,4*S*)-4-methyl-1,2-cyclohexanediaminium D-tartrate **1b**.

Oxalatoplatinum(II) complexes **3a** and **3b** were fully characterized by elemental analysis and multinuclear (¹H, ¹³C, and ¹⁹⁵Pt) one- and two-dimensional NMR spectroscopy. The coordination sphere around the platinum atom can best

be judged by measuring a ^{195}Pt NMR spectrum. The resonance at -365 ppm for **3a** (Figure 2) is indicative for a PtN_2O_2 coordination and is in accordance with the chemical shift found for oxaloplatin at -361 ppm.²⁷ The corresponding ^{195}Pt signal for the dichlorido precursor complex **2a** with

Scheme 1. Synthesis of $\{(1R,2R,4R)\text{-4-Methyl-1,2-cyclohexanediamine}\}$ oxaloplatinum(II), **3a**^a



^a (i) $\text{H}_2\text{O}_2/\text{HCOOH}$, (ii) MsCl/Py , NaN_3 , (iii) Pd/CaCO_3 , H_2 (3 bar), (iv) L-tartaric acid, (v) $\text{K}_2\text{PtCl}_4/\text{NaOH}$ (0.25 M), and (vi) AgNO_3 , potassium oxalate. Structures of 4-ethyl- and 4-*t*-butyl oxaloplatin derivatives **4** and **5**, synthesized as enantiomeric mixtures (all substituents at the cyclohexane ring in equatorial positions).

PtN_2Cl_2 coordination was detected significantly upfield at -644 ppm.

In **3a**, all substituents (two amino and one methyl group) of the cyclohexane ring are in an equatorial position; consequently, protons at carbon atoms 1, 2, and 4 are axially oriented, which can be proven by the Karplus relationship for NMR spin–spin coupling constants (vicinal $\text{H}-\text{C}-\text{C}-\text{H}$ coupling constants are large at angles of 180° with $^3J_{\text{H,H}} \approx 11\text{--}12$ Hz, and small when the torsion angle is 60° with a coupling of around 5 Hz).

Indeed, large couplings of the axial proton H-1ax at 2.31 ppm with the neighboring protons H-2ax and H-6ax with $^3J_{\text{H,H}} = 11.5$ Hz, and a small $^3J_{\text{H,H}}$ coupling to H-6eq of 4 Hz were detected (Figure 2), proving the equatorial position of the amino substituent. The same holds true for proton H-2ax, demonstrating the trans-configuration at C1–C2. In the case of proton H-3ax, resonating at 0.89 ppm, a quartet with a coupling constant of 12 Hz was found as a result of two neighboring axial protons (H-2ax, and H-4ax) and additionally the large geminal $^3J_{\text{H,H}}$ coupling to proton H-3eq. Axial position of H-4ax finally proves that the methyl group at C-4 is equatorially oriented. Signal assignment of all remaining protons is based on two-dimensional ^1H , ^1H - and ^1H , ^{13}C correlated NMR spectra. Of note is the diastereotopic splitting of the methylene protons at C-3, C-4, and C-6, giving rise to six single shift correlation signals in the ^1H , ^{13}C NMR spectrum. Synthesis and characterization of racemic 4-ethyl and 4-*t*-butyl-1,2-cyclohexanediamine}oxaloplatinum(II) complexes **4** and **5** (all substituents at the cyclohexane ring equatorial position, Scheme 1) were described recently.²⁸

With the intention of further optimizing structure–activity relationships, the platinum complex **3c**, $\{(1R,2R,4S)\text{-4-methyl-1,2-cyclohexanediamine}\}$ oxaloplatinum(II), exhibiting

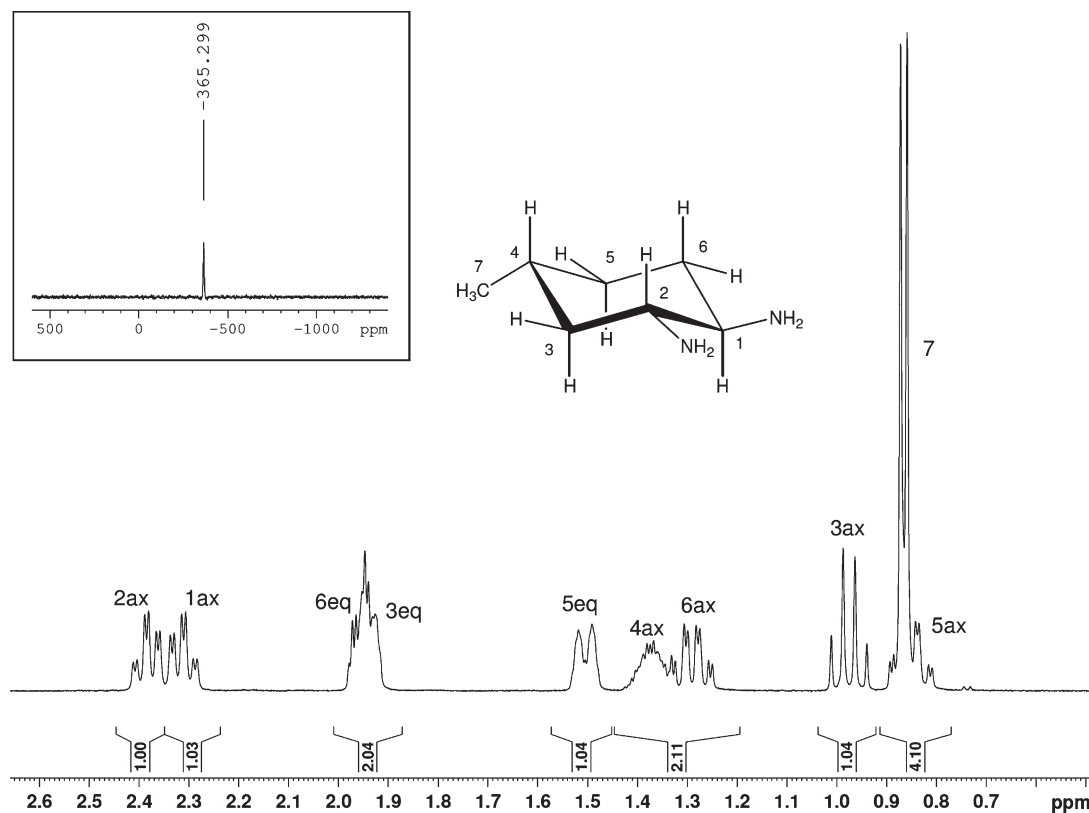
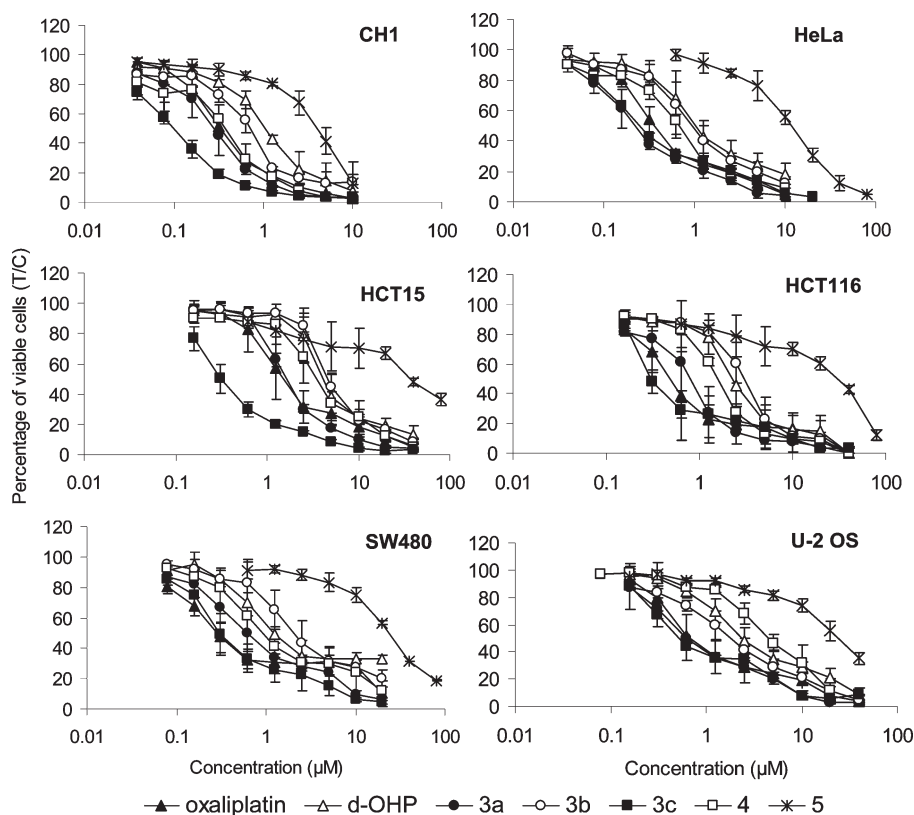


Figure 2. ^1H and ^{195}Pt (small insert) NMR spectrum of $\{(1R,2R,4R)\text{-4-methyl-1,2-cyclohexanediamine}\}$ oxaloplatinum(II) **3a** with NMR numbering scheme and signal assignment. The oxaloplatinum(II) fragment has been omitted for clarity.

Table 1. Cytotoxicity of Oxaliplatin Derivatives Compared to Oxaliplatin in Six Human Cancer Cell Lines

compd	IC ₅₀ (μM) ^a					
	CH1	HeLa	HCT-15	HCT-116	SW480	U-2 OS
oxaliplatin	0.33 ± 0.09	0.35 ± 0.07	1.5 ± 0.6	0.38 ± 0.03	0.30 ± 0.08	0.72 ± 0.24
d-OHP ^b	1.0 ± 0.04	1.1 ± 0.4	4.4 ± 1.6	1.7 ± 0.1	1.3 ± 0.3	2.5 ± 0.7
3a	0.28 ± 0.09	0.21 ± 0.06	1.6 ± 0.1	0.81 ± 0.31	0.67 ± 0.31	0.71 ± 0.41
3b	0.69 ± 0.10	0.88 ± 0.38	4.6 ± 0.7	2.9 ± 0.7	2.3 ± 1.2	1.8 ± 0.6
3c	0.10 ± 0.01	0.24 ± 0.02	0.33 ± 0.07	0.32 ± 0.05	0.33 ± 0.14	0.52 ± 0.03
4	0.38 ± 0.08	0.66 ± 0.13	3.4 ± 1.0	1.6 ± 0.1	0.92 ± 0.30	4.0 ± 0.3
5	4.1 ± 0.8	11 ± 2	39 ± 3	31 ± 2	24 ± 3	24 ± 5

^a 50% inhibitory concentrations in the MTT assay (96 h exposure). Values are means ± standard deviations obtained from at least two (mostly three) independent experiments. ^b d-OHP is the (1*S*,2*S*)-enantiomer of oxaliplatin.

**Figure 3.** Concentration–effect curves of ring-substituted oxaliplatin derivatives in comparison to oxaliplatin and its *S,S* analogue (d-OHP) in CH1, HeLa, U-2 OS, HCT-15, HCT-116, and SW480 cells, obtained by the MTT assay (96 h exposure).

an axial methyl substituent at position 4 of the cyclohexane ring, was synthesized (Supporting Information, Scheme S2). Starting from enantiomerically pure (*S*)-citronellal, (*S*)-4-methylcyclohexene was prepared, which was converted to the corresponding diazide exhibiting trans-configuration at C1/C2. After reduction, (1*R*,2*R*,4*S*)-4-methyl-1,2-cyclohexanediaminium L-tartrate, **1c**, was obtained (diastereomeric purity was proven by chiral HPLC in the form of the Cbz derivative, Supporting Information, Figure S3). In analogy to **3a** and **3b**, the oxalato complex **3c** was synthesized and characterized. Besides a distinctly different ¹⁹⁵Pt chemical shift (**3c**, −381 ppm; **3a**, −365 ppm), the axial position of the methyl group could be judged by comparison of ¹H (Supporting Information, Figure S4) and ¹³C NMR spectra of **3a** and **3c**, respectively. As expected, the chemical shift difference of protons H-1ax and H-2ax ($\Delta\delta$ = 0.27 ppm) in **3c** is significantly bigger compared to **3a** ($\Delta\delta$ = 0.08 ppm). The same holds true for chemical shift differences of carbon atoms C1 and C2 in **3c** ($\Delta\delta$ = 4.9 ppm) and **3a** ($\Delta\delta$ = 0.2 ppm). However, most indicative are the differences (shapes

and chemical shifts, compare Figures 2 and Supporting Information, Figure S4) in the proton NMR spectra for ¹H resonances at C3, C4 and C5.

Cytotoxicity in Cancer Cell Lines and Structure–Activity Relationships. Cytotoxicity of oxaliplatin and the here presented derivatives with equatorial alkyl substituents in position 4 of the cyclohexane ring was compared by means of a colorimetric microculture assay (MTT assay) in six human cancer cell lines representing four tumor entities: ovarian carcinoma (CH1), cervical carcinoma (HeLa), osteosarcoma (U-2 OS), and colon carcinoma (HCT-15, HCT-116, SW480), yielding IC₅₀ values mostly in the low micromolar or even submicromolar range (Table 1, Figure 3).

Oxaliplatin and the 4-methyl derivative **3a** show quite similar cytotoxic potencies in all six cell lines. Notably, **3a** is at least as active as oxaliplatin in four of them, except for the two colon cancer cell lines HCT-116 and SW480. Generally, the (1*R*,2*R*,4*R*)-enantiomer **3a** is by factors of 2–4 more cytotoxic than the (1*S*,2*S*,4*S*)-enantiomer **3b**, indicating that the well-known structure–activity relationship observed

Table 2. Cytotoxicity of Oxaliplatin Derivatives Compared to Oxaliplatin in Cisplatin- And Oxaliplatin-Resistant Human Cancer Cell Models

compd	IC ₅₀ (μM) ^a								
	GLC4	GLC4/CDDP	-fold resistance	A2780	A2780/cis	-fold resistance	HCT116	HCT116 oxR	-fold resistance
cisplatin	1.7 ± 0.5	18.0	10.6	1.8 ± 0.2	> 10	> 5	4.7 ± 0.1	7.3 ± 0.1	1.6
oxaliplatin	0.6 ± 0.2	1.2 ± 0.3	2.0	0.4 ± 0.2	0.7 ± 0.4	1.8	0.6 ± 0.1	22.0 ± 0.1	36.7
3a	0.8 ± 0.1	2.1 ± 0.1	2.6	0.5 ± 0.1	1.6 ± 0.8	3.2	1.5 ± 0.1	11.7 ± 0.1	7.8
3c	0.3 ± 0.2	0.6 ± 0.1	2.0	0.2 ± 0.1	0.5 ± 0.3	2.5	0.5 ± 0.1	9.3 ± 0.1	18.6

^a 50% inhibitory concentrations in the MTT assay (72 h exposure). Values are means ± standard deviations obtained from at least two (mostly three) independent experiments.

with oxaliplatin and its (1*S*,2*S*)-enantiomer (d-OHP) also applies to the alkyl-substituted derivatives. The other 4-methyl derivative **3c** (methyl substituent in axial position) is even more cytotoxic than oxaliplatin in the majority of cell lines and thus the most potent of the studied compounds, whereas the racemic 4-ethyl derivative **4** yields IC₅₀ values that are mostly intermediate between those of **3a** and **3b** (with the exception of U-2 OS cells).

In contrast, the IC₅₀ values of the racemic 4-*t*-butyl derivative **5** are on average an order of magnitude higher than those of **4**. These data support a previous study, which showed that large alkyl substituents will result in a decrease of cytotoxicity.²⁹ Generally, the cytotoxicity profiles of these compounds resemble each other, with CH1 and HeLa being the most sensitive cell lines and HCT-15 being the least sensitive cell line. Therefore, fundamental differences in the underlying molecular mechanisms of action are unlikely.

The cytotoxic properties of compounds **3a** and **3c** were also analyzed in cisplatin- and oxaliplatin-resistant cell models derived from small cell lung (GLC4), ovarian cancer (A2780), and colon cancer (HCT-116) (Table 2). Both highly cisplatin-resistant cell models (GLC4/CDDP and A2780/cis) were (comparable to oxaliplatin) significantly but very moderately (up to 3.2-fold) cross-resistant to the novel derivatives. The resistance of oxaliplatin-insensitive HCT-116 oxR against the new derivatives was, as expected, more distinct (up to 18.6-fold) as compared to that of cisplatin. Nevertheless, it was significantly weaker for both tested derivatives (**3a** and **3c**) as compared to oxaliplatin (36.7-fold).

In Vivo Anticancer Activity. Anticancer activity in vivo was investigated in the murine L1210 leukemia model. Compounds were administered intraperitoneally on three consecutive days. A transient decrease of body weight to not less than 85% was considered tolerable, and for each compound the tolerable dose resulting in the highest increase in life span (ILS) was considered optimal. Except for **5**, which did not allow dose escalation beyond 12 mg/kg/day because of much lower solubility, the maximum tolerated dose (MTD) was reached for all compounds. The optimal dose in terms of therapeutic efficacy is mostly identical with the MTD, except for d-OHP, the (*S,S*)-analogue of oxaliplatin (Table 3). Remarkably, a mere 50% dose increase over the MTD (6 mg/kg/day) turned oxaliplatin in a 100% lethal compound, indicating a steep lethality curve, whereas in the case of the new derivatives, a 50% increase over the respective MTD resulted only in 0–2 toxic deaths (in groups of six animals each). With the exception of **3b**, all compounds were tolerated in at least 50% higher doses (9 mg/kg/day) than oxaliplatin.

All compounds tested prolonged the survival of leukemic mice with high statistical significance ($p < 0.001$) but to different extents. The optimal therapeutic effect of the parent compound oxaliplatin caused an increase in life-span (ILS) by 152% and long-term survival of two animals (Table 3,

Figure 4A). Although in equal doses the efficacy of the 4-methyl derivative **3a** is not higher than that of oxaliplatin, the lower toxicity of this compound enables the application of a higher dose, resulting in a clearly superior therapeutic effect with as much as five long-term survivors and an ILS of more than 200% (Figure 4B). Surprisingly, the analogous complex **3c** (with the 4-methyl substituent in axial instead of equatorial position) causes an ILS of only 122%. Thus, this compound is much less active than **3a** and even somewhat less active than oxaliplatin despite a cytotoxic potency superior to all other compounds studied in vitro. The 4-ethyl derivative **4** is also slightly less effective than oxaliplatin and causes an ILS of 129%, with one long-term surviving animal at the optimal dose. However, this compound is a racemic mixture, and improved therapeutic efficacy might still be expected from the pure (1*R*,2*R*,4*R*)-enantiomer. The lower efficacy of (1*S*,2*S*)-enantiomers is confirmed by data obtained with d-OHP and **3b**, which are no more than half as effective as oxaliplatin and **3a**, respectively. Finally, further increasing the size of the substituent to *t*-butyl (compound **5**) results in a tremendous loss of activity in applicable doses, which parallels the structure–activity relationships observed in vitro.

A synopsis of in vitro and in vivo data reveals that small alkyl substituents (methyl, perhaps also ethyl) on the cyclohexane ring result in an optimum with respect to the therapeutic index mainly due to a higher tolerability than unsubstituted oxaliplatin and a higher activity than derivatives with larger substituents. However, the geometric orientation (axial vs equatorial) of the substituent obviously plays a decisive role, having opposite effects on cytotoxicity in vitro and efficacy in vivo. Apart from that, structure–activity relationships in vitro and in vivo nicely parallel each other within the 4-substituted oxaliplatin derivatives, but this aberrant example demonstrates that caution should be exercised when selecting candidate compounds for drug development on the basis of in vitro data. The L1210 leukemia model employed may seem remote from the actual clinical indication of oxaliplatin, i.e. colorectal cancer, but it should be called in mind that it was one of the few tumor models in which the promising activity of oxaliplatin was originally recognized and therefore proved particularly valuable in this context.^{30,31} Nevertheless, further evaluation of the compounds will require additional models, in particular, solid tumors.

As the cytotoxicity profiles of the studied compounds argue against fundamental differences in the mode of action, the reasons for the differences in therapeutic index and the favorable cross-resistance patterns may be found in the combination of characteristics such as lipophilicity and bulkiness and their subtle consequences for drug transport, biotransformation, and interactions with DNA as well as DNA repair systems.

Comparing both methyl derivatives **3a** (equatorial methyl group) and **3c** (axial methyl group), it is remarkable that **3c** is

Table 3. Tolerability and Efficacy of Intraperitoneal Treatment with Oxaliplatin Derivatives Compared to Oxaliplatin in L1210 Leukemia-Bearing Mice (Therapeutic Effects at the Respective Optimum Dose Are Marked in Bold Type)

compd	dose (mg/kg/day)	min body weight (%)	toxic deaths	ILS (%) ^a	long-term survivors ^b
oxaliplatin	9		6/6		0/6
	6 (MTD) ^c	93.2	0/6	152	2/6
	4.5	91.3	0/6	89	1/6
	3	94.1	0/6	94	1/6
d-OHP	12		1/6		0/6
	9 (MTD) ^c	85.9	0/6	63	0/6
	6	93.1	0/6	73	1/6
	4.5	93.6	0/6	26	0/6
3a	12		2/6		4/6
	9 (MTD) ^c	88.6	0/6	> 200	5/6
	6	97.5	0/6	119	0/6
	4.5	94.6	0/6	84	1/6
	3	97.3	0/6	90	0/6
3b	9		1/6		0/6
	6 (MTD) ^c	92.0	0/6	103	1/6
	4.5	93.4	0/6	68	2/6
	3	97.9	0/6	68	1/6
3c	12		2/6		1/6
	9 (MTD) ^c	86.4	0/6	122	2/6
	6	87.3	0/6	78	1/6
	4.5	87.9	0/6	111	2/6
4	12	83.2	0/6	144	2/6
	9 (MTD) ^c	89.9	0/6	129	1/6
	6	93.6	0/6	89	0/6
	3	98.4	0/6	61	0/6
5	12	100.0	0/6	33	0/6
	6	100.0	0/6	25	0/6
	3	98.5	0/6	17	0/6

^a Increase in life span compared to untreated controls, based on median survival; all values indicate life prolongation with high statistical significance ($p < 0.001$). ^b Animals with ILS > 200% without any signs of leukemia. ^c Maximum tolerated dose.

equipped with a higher cytotoxicity in vitro, but in parallel showing a lower anticancer activity in vivo. Differences between **3a** and **3c** in the cellular accumulation and DNA adduct formation are expected to be very similar in vitro and in vivo. Nevertheless, one might assume the existence of interacting factors like altered transport by drug uptake and/or efflux pumps which might impact on the pharmacological characteristics of these stereoisomeric complexes in vivo but not in vitro. The identification of these interacting factors is a matter of ongoing investigations.

Conclusions

In this study, we successfully developed an oxaliplatin derivative with enhanced antitumor activity compared to the parental drug by introducing a small alkyl substituent on the cyclohexane ring in equatorial position. Using the L1210 murine leukemia model, the highest anticancer activity was proven for {(1*R*,2*R*,4*R*)-4-methyl-1,2-cyclohexanediamine}oxalatoplatinum(II), resulting in both increased life span and enhanced long-term survival. Although in vitro this compound is not consistently more cytotoxic than oxaliplatin, the better tolerability enables application of higher doses, resulting in enhanced efficacy in vivo. Considering that adverse effects are a central problem of clinical oxaliplatin application, the evaluation of the new derivative in (pre)clinical studies is highly desirable. These studies should

primarily focus on colorectal cancer, where oxaliplatin is used as therapeutic standard, but also on other tumors recently suggested to be sensitive against this third-generation platinum compound like certain leukemias³² or esophago-gastric cancer.³³

Experimental Section

If necessary, the reactions were carried out in dry solvents and under argon atmosphere. Potassium tetrachloridoplatinate(II) was obtained from Johnson Matthey (Switzerland). All other chemicals obtained from commercial suppliers were used as received and were of analytical grade. Water was prior to use doubly distilled. The synthetic procedures were carried out in light protected environment when platinum complexes were involved. ¹H, ¹³C, ¹⁵N, ¹⁹⁵Pt, and two-dimensional COSY NMR spectra were recorded with a Bruker Avance DPX 400 instrument (Ultrashield Magnet) at 400.13 MHz (¹H) and 100.63 MHz (¹³C) or with a Bruker Avance III 500 MHz NMR spectrometer at 500.32 (¹H), 125.81 (¹³C), 107.55 (¹⁹⁵Pt), and 50.70 MHz (¹⁵N) in DMF-*d*₇, D₂O, or CDCl₃ at 298 K. ¹⁵N chemical shifts were referenced relative to external NH₄Cl, whereas ¹⁹⁵Pt chemical shifts were referenced relative to external K₂[PtCl₄]. HPLC analysis was carried out using a Dionex Summit system. The sample concentration was 1.0 mg/mL, with an injection volume of 10 μL introduced onto a Chiralcel OD column (250 mm × 4.6 mm) protected by a guard column (50 mm × 4.6 mm) at 5 °C. The flow rate of the mobile phase (hexane:*i*-propyl alcohol 9:1) was 1 mL/min. Melting points were determined with a Büchi B-540 apparatus and are

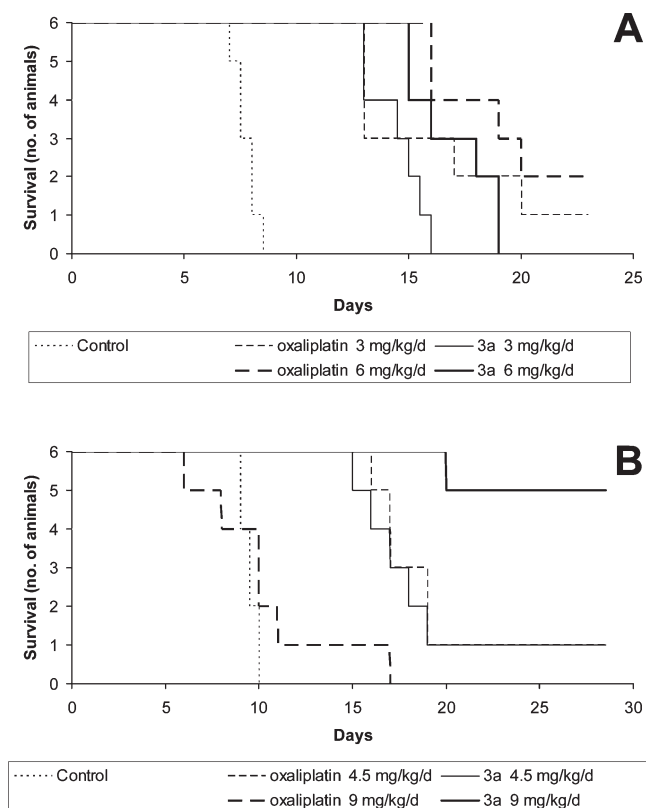


Figure 4. Kaplan–Meier plots showing the survival (days after tumor implantation) of L1210 leukemia-bearing mice treated intraperitoneally with different doses of oxaliplatin or **3a** in comparison to untreated controls, in groups of six animals each. Note that mortality in animals treated with 9 mg/kg/day oxaliplatin is drug-related in all cases (A), whereas the same dose of **3a** results in long-term survival of five animals (B).

uncorrected. Electrospray ionization mass spectra were recorded on a Bruker esquire₃₀₀₀ in positive ion mode. Elemental analyses of prepared compounds were carried out on a Perkin-Elmer 2400 CHN elemental analyzer or a Carlo Erba microanalyzer at the Microanalytical Laboratory of the University of Vienna and are within $\pm 0.4\%$ of the calculated values, confirming their $\geq 95\%$ purity. Silica gel (Polygram SIL G/UV₂₅₄) was used for thin layer chromatography.

(SP-4-3)-[(1R,2R,4R)-4-Methyl-1,2-cyclohexanediamine- κ^2N,N'][ethanedioato(2-)- $\kappa^2O1,O2$]platinum(II) **3a.** AgNO₃ (167 mg, 0.98 mmol) was added to a suspension of (SP-4-3)-dichlorido-[(1R,2R,4R)-4-methyl-1,2-cyclohexanediamine- κ^2N,N']platinum(II) **2a** (200 mg, 0.5 mmol) in water (3 mL). The reaction mixture was stirred for 24 h at room temperature, the precipitated silver chloride was filtered off, and an in situ prepared solution of potassium oxalate from oxalic acid dihydrate (61 mg, 0.48 mmol) and KOH (0.96 mL, 0.5 M, 0.48 mmol) in water (2 mL) was added to the diaqua complex. The reaction mixture was stirred for 24 h at room temperature, the solvent was removed in vacuum, and the pure white complex was obtained after recrystallization in water (1 mL). The product was filtered off and dried under reduced pressure over P₄O₁₀. Yield: 0.82 mg (39%), mp 282–290 °C (decomp). Elemental analysis, Found: C, 26.05; H, 3.65; N, 6.55. Calcd for C₉H₁₆N₂O₄Pt: C, 26.28; H, 3.92; N, 6.81. MS (ESI⁺) m/z 434 [M + Na]⁺. ¹H NMR in D₂O: δ = 0.85 (dq, ³J_{H,H} = ²J_{H,H} = 13 Hz, ³J_{H,H} = 3.5 Hz, 1H, H-5ax), 0.86 (d, ³J_{H,H} = 6.5 Hz, 3H, H-7), 0.98 (q, ³J_{H,H} = ²J_{H,H} = 12 Hz, 1H, H-3ax), 1.29 (dddd, J_{H,H} = 12.5 Hz, J_{H,H} = 12.5 Hz, J_{H,H} = 12.0 Hz, J_{H,H} = 3.5 Hz, 1H, H-6ax), 1.37 (m, 1H, H-4ax), 1.51 (m, 1H, H-5eq), 1.88–2.00 (m + m, 2H, H-3eq, H-6eq), 2.31 (dt, ³J_{H,H} = 11.5 Hz, ³J_{H,H} = 4.0 Hz, 1H, H-1ax), 2.39 (dt, ³J_{H,H} = 11.5 Hz,

³J_{H,H} = 4.0 Hz, 1H, H-2ax). ¹³C NMR in D₂O: δ = 20.0 (C-7), 30.6 (C-6), 30.9 (C-4), 32.2 (C-5), 39.5 (C-3), 62.0 (C-2), 62.2 (C-1), 168.3 (COO). ¹⁹⁵Pt NMR in D₂O: δ = –365.

(SP-4-3)-[(1S,2S,4S)-4-Methyl-1,2-cyclohexanediamine- κ^2N,N'][ethanedioato(2-)- $\kappa^2O1,O2$]platinum(II) **3b.** Following the same procedure as described for **3a**, complex **3b** was obtained from (SP-4-3)-dichlorido-[(1S,2S,4S)-4-methyl-1,2-cyclohexanediamine- κ^2N,N']platinum(II) **2b** (200 mg, 0.5 mmol). Yield: 0.82 mg (38%), mp 275–280 °C (decomp). Elemental analysis, Found: C, 26.07; H, 3.66; N, 6.83. Calcd for C₉H₁₆N₂O₄Pt: C, 26.28; H, 3.92; N, 6.81. MS (ESI⁺) m/z 434 [M + Na]⁺. ¹H NMR in D₂O: δ = 0.85 (dq, ³J_{H,H} = ²J_{H,H} = 13 Hz, ³J_{H,H} = 3.5 Hz, 1H, H-5ax), 0.86 (d, ³J_{H,H} = 6.5 Hz, 3H, H-7), 0.97 (q, ³J_{H,H} = ²J_{H,H} = 12 Hz, 1H, H-3ax), 1.28 (dddd, J_{H,H} = 12.5 Hz, J_{H,H} = 12.5 Hz, J_{H,H} = 12.0 Hz, J_{H,H} = 3.5 Hz, 1H, H-6ax), 1.36 (m, 1H, H-4ax), 1.50 (m, 1H, H-5eq), 1.88–2.00 (m + m, 2H, H-3eq, H-6eq), 2.30 (dt, ³J_{H,H} = 11.5 Hz, ³J_{H,H} = 4.0 Hz, 1H, H-1ax), 2.38 (dt, ³J_{H,H} = 11.5 Hz, ³J_{H,H} = 4.0 Hz, 1H, H-2ax). ¹³C NMR in D₂O: δ = 20.0 (C-7), 30.6 (C-6), 30.9 (C-4), 32.2 (C-5), 39.5 (C-3), 62.0 (C-2), 62.2 (C-1), 168.3 (COO). ¹⁹⁵Pt NMR in D₂O: δ = –365.

(SP-4-3)-[(1R,2R,4S)-4-Methyl-1,2-cyclohexanediamine- κ^2N,N'][ethanedioato(2-)- $\kappa^2O1,O2$]platinum(II) **3c.** (SP-4-3)-[Dichlorido-[(1R,2R,4S)-4-methyl-1,2-cyclohexanediamine- κ^2N,N']platinum(II)] (1.767 g, 4.48 mmol) was suspended in 80 mL of water and a solution of AgNO₃ (1.462 g, 8.60 mmol) in 10 mL of water was added. The suspension was stirred for 24 h at room temperature. The AgCl formed was filtered off with a G4 glass sinter filter with an additional MN GF3 filter. The clear, slightly yellowish solution was treated with conditioned basic ion-exchange resin IRA402 for 24 h at room temperature (shaking). [Conditioning of IRA402: 150 g of IRA402 chloride form was stirred with 2 M NaOH (400 mL) for 30 min. Then the resin was washed with deionized water until achieving neutral pH followed by washing with distilled water twice.] The ion-exchange resin was separated from the solution by decantation and washed with water three times. The combined aqueous solutions were filtered through a G4 glass sinter filter, and oxalic acid dihydrate (0.565 g, 4.48 mmol) was added. The mixture was put into a round flask, and the volume was reduced to ca. 80 mL within 3 h, whereupon the liquid became cloudy. The latter was kept at room temperature for 12 h and was further reduced to ca. 40 mL. A white solid formed which was finally filtered with a G4 glass sinter filter after 1 h, washed with water twice, and dried in vacuum over P₄O₁₀. Yield: 0.534 g (29%). Elemental analysis, Found: C, 26.07; H, 3.88; N, 6.66. Calcd for C₉H₁₆N₂O₄Pt: C, 26.28; H, 3.92; N, 6.81. ¹H NMR in D₂O: δ = 0.84 (d, ³J_{H,H} = 7.5 Hz, 3H, H-7), 1.22–1.55 (m + m + m + m, 4H, H-5eq, H-5ax, H-3ax, H-6ax) 1.71–1.90 (m + m + m, 3H, H-3eq, H-6eq, H-4eq), 2.24 (dt, ³J_{H,H} = 12.0 Hz, ³J_{H,H} = 4.5 Hz, 1H, H-1ax), 2.51 (dt, ³J_{H,H} = 12.0 Hz, ³J_{H,H} = 4.0 Hz, 1H, H-2ax). ¹³C NMR in D₂O: δ = 16.7 (C-7), 26.4 (C-6), 27.0 (C-4), 29.3 (C-5), 37.2 (C-3), 57.8 (C-2), 62.7 (C-1), 168.3 (COO). ¹⁹⁵Pt NMR in D₂O: δ = –381.

Cell Lines and Culture Conditions. CH1 (ovarian carcinoma, human) cells were kindly provided by Lloyd R. Kelland (CRC Centre for Cancer Therapeutics, Institute of Cancer Research, Sutton, UK). HeLa (cervical carcinoma, human) and U-2 OS (osteosarcoma, human) cells were donated by Thomas Czerny (Institute of Genetics, University of Veterinary Medicine Vienna, Austria). SW480, HCT116, and HCT15 (all colon carcinoma, human) cells were kindly provided by Brigitte Marian (Institute of Cancer Research, Medical University of Vienna, Austria). In addition, cell models comprising a parental drug-sensitive and respective cisplatin- or oxaliplatin-resistant subline were used. GLC4 small cell lung cancer cells together with cisplatin-resistant GLC4/CDDP cells were kindly supplied by Elisabeth de Vries, University of Groningen. The ovarian carcinoma cell line A2780 together with the cisplatin-resistant subline A2780/cis were obtained from Sigma. The oxaliplatin-resistant subline HCT-116 oxR was established by stepwise drug selection of HCT-116 colon cancer cells.

GLC4 and A2780 cell lines and derivatives were grown in RPMI1680 medium with 10% fetal bovine serum. All other cells

were cultured in complete culture medium, i.e., Minimal Essential Medium (MEM) supplemented with 10% heat-inactivated fetal bovine serum, 1 mM sodium pyruvate, 4 mM L-glutamine, and 1% nonessential amino acids (100×) (all purchased from Sigma-Aldrich). Cultures were maintained at 37 °C in a humidified atmosphere containing 5% CO₂ and 95% air.

Cytotoxicity Tests in Cancer Cell Lines. Antiproliferative activity was determined by a colorimetric microculture assay (MTT assay, MTT = 3-(4,5-dimethyl-2-thiazolyl)-2,5-diphenyl-2H-tetrazolium bromide). For this purpose, cells were harvested from culture flasks by trypsinization and seeded in 100-μL aliquots into 96-well microculture plates (Iwaki/Asahi Technoglass) in the following densities: 1.5×10^3 (CH1, HeLa), 2.0×10^3 (GLC4 cell model), 2.5×10^3 (SW480, HCT-116 cell model, HCT-15), and 3.2×10^3 (U2OS, A2780 cell model) viable cells/well. Cells were allowed to settle and resume adherent growth in drug-free complete culture medium for 24 h, followed by the addition of dilutions of the test compounds in 100 μL/well complete culture medium and incubation for 96 h. In experiments involving drug-resistance models, the incubation time was 72 h. At the end of exposure, medium was replaced by 100 μL/well RPMI 1640 medium (supplemented with 10% heat-inactivated fetal bovine serum and 4 mM L-glutamine) plus 20 μL/well MTT solution in phosphate-buffered saline (5 mg/mL). After incubation for 4 h, medium was removed and the formazan product formed by viable cells was dissolved in DMSO (150 μL/well). Optical densities at 550 nm were measured with a microplate reader (Tecan Spectra Classic). The quantity of viable cells was expressed in terms of *T/C* values by comparison to untreated controls, and 50% inhibitory concentrations (IC₅₀) were calculated from concentration–effect curves by interpolation. Evaluation is based on means from at least two (mostly three) independent experiments, each comprising six replicates per concentration level.

Antileukemic Activity in Vivo. Animal experiments were performed in accordance with the European Community Guidelines for the use of experimental animals in the animal facility at the Cancer Research Institute, Slovak Academy of Sciences, Bratislava, Slovak Republic. L1210 murine leukemia cells (1×10^5) were injected in a volume of 0.5 mL into DBA/2J mice (weighing 18–22 g) intraperitoneally on day 0. The test compounds were administered intraperitoneally in a volume of 0.5 mL aqua ad injectionem per mouse per day in a split-dose regimen (days 1, 2, and 3 after implantation of cells) to groups of six animals per dose. Toxicity of the test compounds was monitored by daily observation of animals and registration of their body weight. Therapeutic efficacy of the test compounds was monitored by recording the lengths of survival of experimental mice compared to untreated control animals. The experiment was terminated after the 3-fold of the survival time of untreated controls, and animals experiencing an increase in life span of more than 200% without any signs of leukemia were considered long-term survivors. The absence of malignant disease in the abdominal cavity was confirmed by dissection. Statistical significance of survival data was calculated using the unpaired *t* test.

Acknowledgment. We are indebted to the FFG–Austrian Research Promotion Agency (811591), the Austrian Council for Research and Technology Development (IS526001), the FWF (Austrian Science Fund), and COST D39.

Supporting Information Available: Figure with the crystal structure of an oxaliplatin 1,2-d(GpG) intrastrand cross-link in a DNA dodecamer duplex; scheme with the separation of racemic (1*R*,2*R*,4*R*/(1*S*,2*S*,4*S*))-4-methyl-1,2-cyclohexanediamine and with structures of CBz analogues used for chiral HPLC analysis, figure with the confirmation of enantiomeric purity of (1*R*,2*R*,4*R*)- and (1*S*,2*S*,4*S*))-4-methyl-1,2-cyclohexanediamine by chiral HPLC, scheme with the synthesis

of {(1*R*,2*R*,4*S*))-4-methyl-1,2-cyclohexanediamine}oxalatoplatinum(II), figure with the confirmation of diastereomeric purity of (1*R*,2*R*,4*S*))-4-methyl-1,2-cyclohexanediamine after transformation into the CBz-derivative, figure with ¹H- and ¹⁹⁵Pt NMR spectra of {(1*R*,2*R*,4*S*))-4-methyl-1,2-cyclohexanediamine}oxalatoplatinum(II) **3c**, synthesis and characterization of (S)-4-methylcyclohexene, 4-methyl-1,2-cyclohexanediaminium tartrates **1a–1c**, (SP-4-3)-dichlorido[4-methyl-1,2-cyclohexanediamine-κ²N,N']platinum(II) complexes **2a–2c**, and N,N'-bis-(benzyloxycarbonyl)-4-methyl-1,2-cyclohexanedicarbamates **6** and **7**. This material is available free of charge via the Internet at <http://pubs.acs.org>.

References

- (1) Lippert, B.; Ed., *Cisplatin: Chemistry and Biochemistry of a Leading Anticancer Drug*; Verlag Helvetica Chimica Acta, Zürich and WILEY-VCH, Weinheim, Germany, 1999.
- (2) Rosenberg, B.; VanCamp, L.; Krigas, T. Inhibitor of Cell Division in *Escherichia Coli* by Electrolysis Products From a Platinum Electrode. *Nature* **1965**, *205*, 698–699.
- (3) Rosenberg, B. Platinum Complexes for the Treatment of Cancer. *Interdiscip. Sci. Rev.* **1978**, *3*, 134–147.
- (4) Kidani, Y.; Inagaki, K.; Iigo, M.; Hoshi, A.; Kureitani, K. Antitumor Activity of 1,2-Diaminocyclohexane Platinum Complexes Against Sarcoma-180 Ascites form. *J. Med. Chem.* **1978**, *21*, 1315–1318.
- (5) Galanski, M.; Jakupec, M. A.; Keppler, B. K. Oxaliplatin and derivatives as anticancer drugs—novel design strategies. In: *Metal Compounds in Cancer Chemotherapy*; Pérez, J. M., Fuertes, M. A., Alonso, C., Eds.; Research Signpost: Kerala, India, 2005; pp 155–185.
- (6) O'Dwyer, P. J.; Johnson, S. W. Current Status of Oxaliplatin in Colorectal Cancer. *Semin. Oncol.* **2003**, *30* (3, Suppl 6), 78–87.
- (7) Rixe, O.; Ortuzar, W.; Alvarez, M.; Parker, R.; Reed, E.; Paull, K.; Fojo, T. Oxaliplatin, tetraplatin, cisplatin, and carboplatin: Spectrum of activity in drug-resistant cell lines and in the cell lines of the national cancer institute's anticancer drug screen panel. *Biochem. Pharmacol.* **1996**, *52*, 1855–1865.
- (8) Graham, M. A.; Lockwood, G. F.; Greenslade, D.; Brienza, S.; Bayssas, M.; Gamelin, E. Clinical Pharmacokinetics of Oxaliplatin: A Critical Review. *Clin. Cancer Res.* **2000**, *6*, 1205–1218.
- (9) Kelland, L. The resurgence of platinum-based cancer chemotherapy. *Nature Rev. Cancer* **2007**, *7*, 573–584.
- (10) Eastman, A. The formation, isolation and characterization of DNA adducts produced by anticancer platinum complexes. *Pharmacol. Ther.* **1987**, *34*, 155–166.
- (11) Woyrnarowski, J. M.; Chapman, W. G.; Napier, C.; Herzig, M. C. S.; Juniewicz, P. Sequence- and Region-Specificity of Oxaliplatin Adducts in Naked and Cellular DNA. *Mol. Pharmacol.* **1998**, *54*, 770–777.
- (12) Saris, C. P.; van de Vaart, P. J. M.; Rietbroek, R. C.; Blommaert, F. A. In vitro formation of DNA adducts by cisplatin, lobaplatin and oxaliplatin in calf thymus DNA in solution and in cultured human cells. *Carcinogenesis* **1996**, *17*, 2763–2769.
- (13) Hector, S.; Bolanowska-Higdon, W.; Zdanowicz, J.; Hitt, S.; Pendyala, L. In vitro studies on the mechanism of oxaliplatin resistance. *Cancer Chemother. Pharmacol.* **2001**, *48*, 398–406.
- (14) Fink, D.; Nebel, S.; Aebi, S.; Zheng, H.; Cenni, B.; Nehmé, A.; Christen, R. D.; Howell, S. B. The Role of DNA Mismatch Repair in Platinum Drug Resistance. *Cancer. Res.* **1996**, *56*, 4881–4886.
- (15) Vaisman, A.; Lim, S. E.; Patrick, S. M.; Copeland, W. C.; Hinkle, D. C.; Turchi, J. J.; Chaney, S. G. Effect of DNA Polymerases and High Mobility Group Protein 1 on the Carrier Ligand Specificity for Translesion Synthesis past Platinum–DNA Adducts. *Biochemistry* **1999**, *38*, 11026–11039.
- (16) Paulson, T. G.; Wright, F. A.; Parker, B. A.; Russack, V.; Wahl, G. M. Microsatellite Instability Correlates with Reduced Survival and Poor Disease Prognosis in Breast Cancer. *Cancer. Res.* **1996**, *56*, 4021–4026.
- (17) Spingler, B.; Whittington, D. A.; Lippard, S. J. 2.4 Å Crystal Structure of an Oxaliplatin 1,2-d(GpG) Intrastrand Cross-Link in a DNA Dodecamer Duplex. *Inorg. Chem.* **2001**, *40*, 5596–5602.
- (18) Takahara, P. M.; Rosenzweig, A. C.; Frederick, C. A.; Lippard, S. J. Crystal structure of double-stranded DNA containing the major adduct of the anticancer drug cisplatin. *Nature* **1995**, *377*, 649–652.
- (19) Wu, Y.; Pradhan, P.; Havener, J.; Boysen, G.; Swenberg, J. A.; Campbell, S. L.; Chaney, S. G. J. NMR Solution Structure of an Oxaliplatin 1,2-d(GG) Intrastrand Cross-link in a DNA Dodecamer Duplex. *Mol. Biol.* **2004**, *341*, 1251–1269.

- (20) Bruck, M. A.; Bau, R.; Noji, M.; Inagaki, K.; Kidani, Y. The crystal structures and absolute configurations of the anti-tumor complexes platinum(oxalato)(1*R*,2*R*-cyclohexanediamine) and platinum(malonato)(1*R*,2*R*-cyclohexanediamine). *Inorg. Chim. Acta* **1984**, *92*, 279–284.
- (21) Al-Allaf, T. A. K.; Rashan, L. J.; Steinborn, D.; Merzweiler, K.; Wagner, C. Platinum(II) and palladium(II) complexes analogous to oxaliplatin with different cyclohexyldicarboxylate isomeric anions and their in vitro antitumor activity. Structural elucidation of [Pt(C2O4)(*cis*-dach)]. *Trans. Met. Chem.* **2003**, *28*, 717–721.
- (22) Kido, Y.; Khokhar, A. R.; Al-Baker, S.; Siddik, Z. H. Modulation of cytotoxicity and cellular pharmacology of 1,2-diaminocyclohexane platinum(IV) complexes mediated by axial and equatorial ligands. *Cancer Res.* **1993**, *53*, 4567–4572.
- (23) Pendyala, L.; Kidani, Y.; Perez, R.; Wilkes, J.; Bernacki, R. J.; Creaven, P. J. Cytotoxicity, cellular accumulation and DNA binding of oxaliplatin isomers. *Cancer Lett.* **1995**, *97*, 177–184.
- (24) Boudny, V.; Vrana, O.; Gaucheron, F.; Kleinwachter, V.; Leng, M.; Brabec, V. Biophysical analysis of DNA modified by 1,2-diaminocyclohexane platinum(II) complexes. *Nucleic Acids Res.* **1992**, *20*, 267–272.
- (25) Raju, T. N. The Nobel chronicles. 1988: James Whyte Black, (b 1924), Gertrude Elion (1918–99), and George H. Hitchings (1905–98). *Lancet* **2000**, *355*, 1022–1024.
- (26) Habala, L.; Dworak, C.; Nazarov, A. A.; Hartinger, C. G.; Abramkin, S. A.; Arion, V. B.; Lindner, W.; Galanski, M.; Keppler, B. K. Methyl-substituted *trans*-1,2-Cyclohexanediamines as New Ligands for Oxaliplatin-Type Complexes. *Tetrahedron* **2008**, *64*, 137–146.
- (27) Hoeschele, J. D.; Farrell, N.; Turner, W. R.; Rithner, C. D. Synthesis and characterization of diastereomeric (substituted iminodiacetato)(1,2-diaminocyclohexane)platinum(II) complexes. *Inorg. Chem.* **1988**, *27*, 4106–4113.
- (28) Habala, L.; Galanski, M.; Yasemi, A.; Nazarov, A. A.; Graf von Keyserlingk, N.; Keppler, B. K. Synthesis and structure–activity relationships of mono- and dialkyl-substituted oxaliplatin derivatives. *Eur. J. Med. Chem.* **2005**, *40*, 1149–1155.
- (29) Galanski, M.; Yasemi, A.; Jakupec, M. A.; Keyserlingk, N. Graf v.; Keppler, B. K. Synthesis, cytotoxicity, and structure–activity relationships of new oxaliplatin derivatives. *Monatsh. Chem.* **2005**, *136*, 693–700.
- (30) Kidani, Y.; Noji, M.; Tashiro, T. Antitumor activity of platinum(II) complexes of 1,2-diaminocyclohexane isomers. *Gann.* **1980**, *71*, 637–643.
- (31) Mathé, G.; Kidani, Y.; Noji, M.; Maral, R.; Bourut, C.; Chenu, E. Antitumor activity of l-OHP in mice. *Cancer Lett.* **1985**, *27*, 135–143.
- (32) Tsimberidou, A. M.; Wierda, W. G.; Plunkett, W.; Kurzrock, R.; O'Brien, S.; Wen, S.; Ferrajoli, A.; Ravandi-Kashani, F.; Garcia-Manero, G.; Estrov, Z.; Kipps, T. J.; Brown, J. R.; Fiorentino, A.; Lerner, S.; Kantarjian, H. M.; Keating, M. J. Phase I–II study of oxaliplatin, fludarabine, cytarabine, and rituximab combination therapy in patients with Richter's syndrome or fludarabine-refractory chronic lymphocytic leukemia. *J. Clin. Oncol.* **2008**, *26*, 196–203.
- (33) Cunningham, D.; Starling, N.; Rao, S.; Iveson, T.; Nicolson, M.; Coxon, F.; Middleton, G.; Daniel, F.; Oates, J.; Norman, A. R. Capecitabine and oxaliplatin for advanced esophagogastric cancer. *N. Engl. J. Med.* **2008**, *358*, 36–46.